



# Traveling Wave MRI in a Vertical Bore 21.1-T System

A.A. Tonyushkin<sup>1,2</sup>, J.A. Muniz<sup>3,4</sup>, S.C. Grant<sup>3,4</sup>, A.J.M. Kiruluta<sup>1,2</sup>

<sup>1</sup>Radiology, Massachusetts General Hospital, Boston, MA, <sup>2</sup>Physics, Harvard University, Cambridge, MA, USA

<sup>3</sup>The National High Magnetic Field Laboratory, The Florida State University, Tallahassee, FL, USA

<sup>4</sup>Chemical & Biomedical Engineering, The Florida State University, Tallahassee, FL, USA



## Introduction:

Traveling wave MRI relies on the propagation of temporally and spatially variant RF waves inside a scanner using a waveguide [1], namely the bore/shield of a scanner or a specially constructed metal enclosure. At 7 T, only the lowest TE<sub>11</sub> mode of the cylindrical waveguide can propagate in a hollow bore due to stringent cut-off wavelength requirements [1,2]. However, with the higher fields of pre-clinical animal and vertical magnets, the typical diameter of the open bore is usually small compared to the free-space critical wavelength of the propagating mode in such a waveguide. Under these conditions, other modes of a cylindrical waveguide (hybrid, TM as well as higher order TE modes) are only allowed through the use of high permittivity dielectrics [3,4].

*In this study, a novel partially filled cylindrical dielectric waveguide capable of operating in the traveling wave regime is demonstrated in a vertical 21.1-T ultra-wide bore magnet.* The feasibility of remote imaging for both phantom and tissue samples is displayed for a simple transceive loop coil traveling wave implementation.

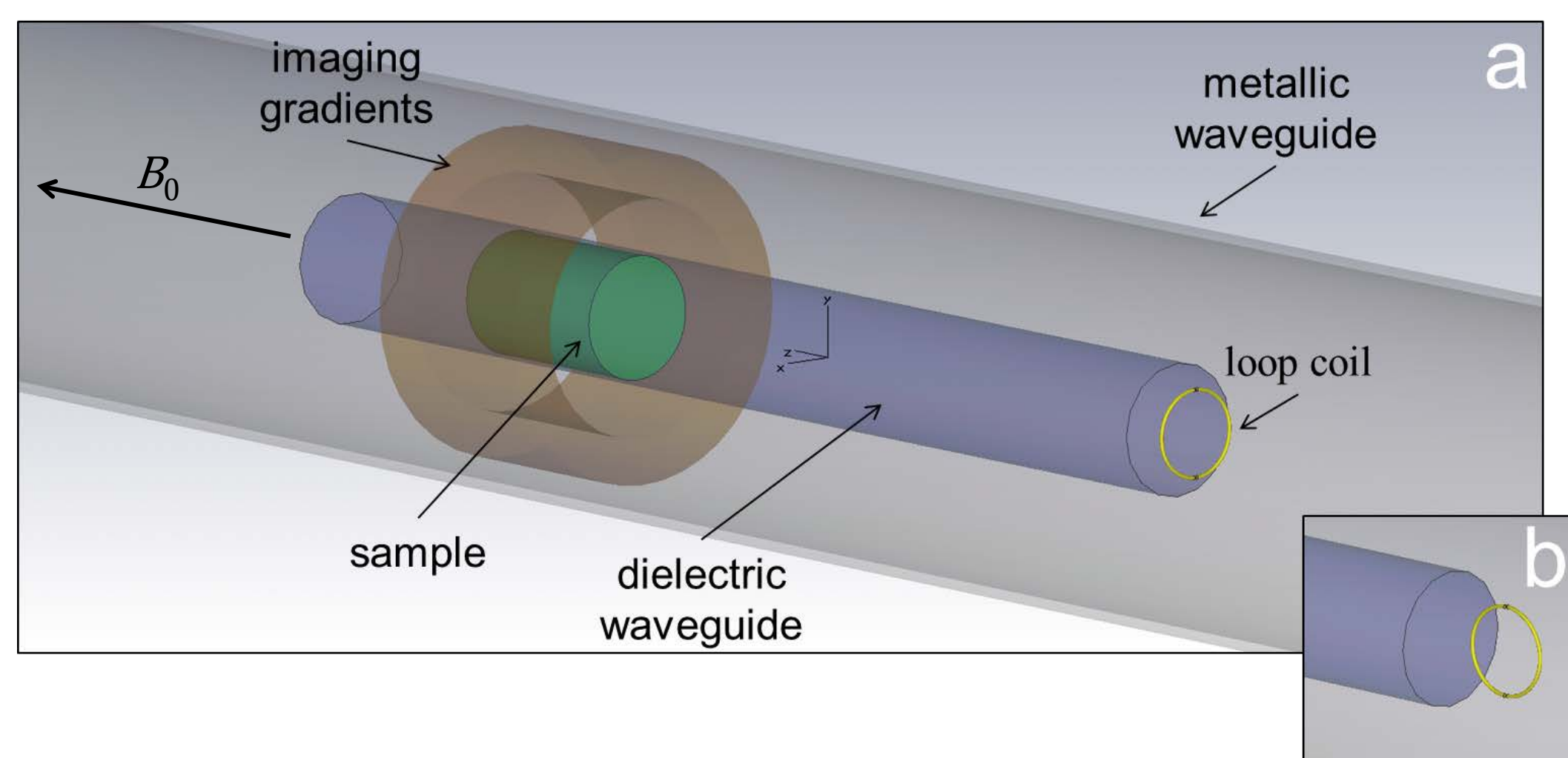


**Fig. 1: Simplified schematic of a cylindrical waveguide for 21.1 T for (a) parallel and (b) orthogonal coil orientations.** Loop coil diameter = 2.4 cm, dielectric waveguide = 3.5-cm OD x 34-cm length, metallic waveguide = 5.5-cm OD, gradients = 6.3-cm ID, distance from coil to sample = 21-24 cm

## Materials & Methods:

- Vertical 21.1 T (900-MHz <sup>1</sup>H Larmor freq,  $\lambda = 33$  cm)
- Available diameter: 6.3-cm ID imaging gradients
- Critical wavelength  $\lambda_{cr} = 18$  cm for the first available TE<sub>11</sub> waveguide mode
- Aqueous samples provide the high permittivity required to modify the cut-off requirements
- Partially filled concentric waveguide (see Fig. 1)
  - Inner waveguide: dielectric composed of deionized water ( $\epsilon_r = 80$ ) with 3.5-cm OD and 33-cm length
  - Outer waveguide: hollow copper waveguide with 5.5-cm OD and 33-cm length
  - Under these conditions, multiple propagation modes are supported with  $\lambda_{cr} > 4.4$  cm

## Electromagnetic Simulations:

- A finite element method (COMSOL Multiphysics) was employed for the screened dielectric waveguide:  $\epsilon_r = 80$ ,  $\sigma = 5 \times 10^{-5}$  S/m

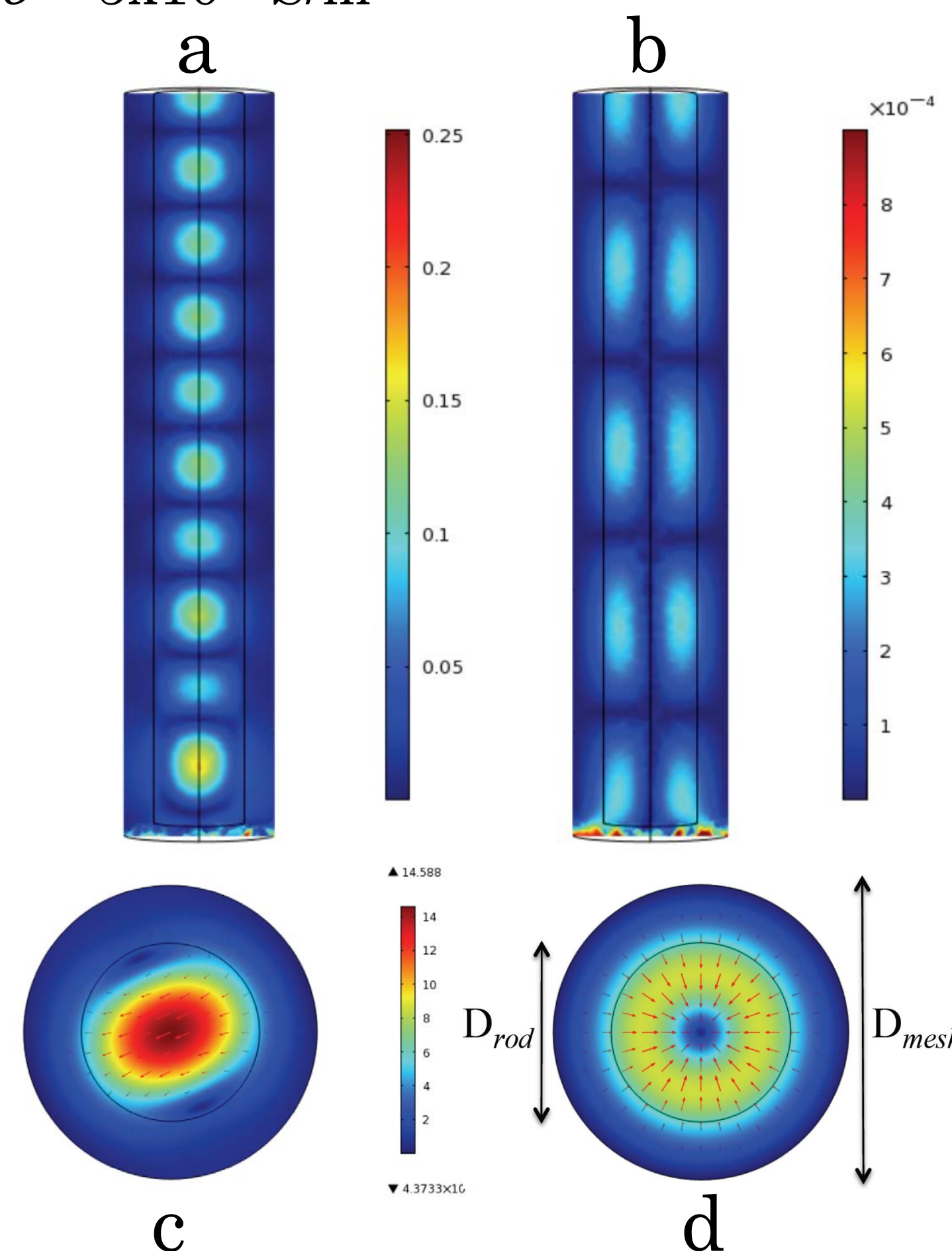
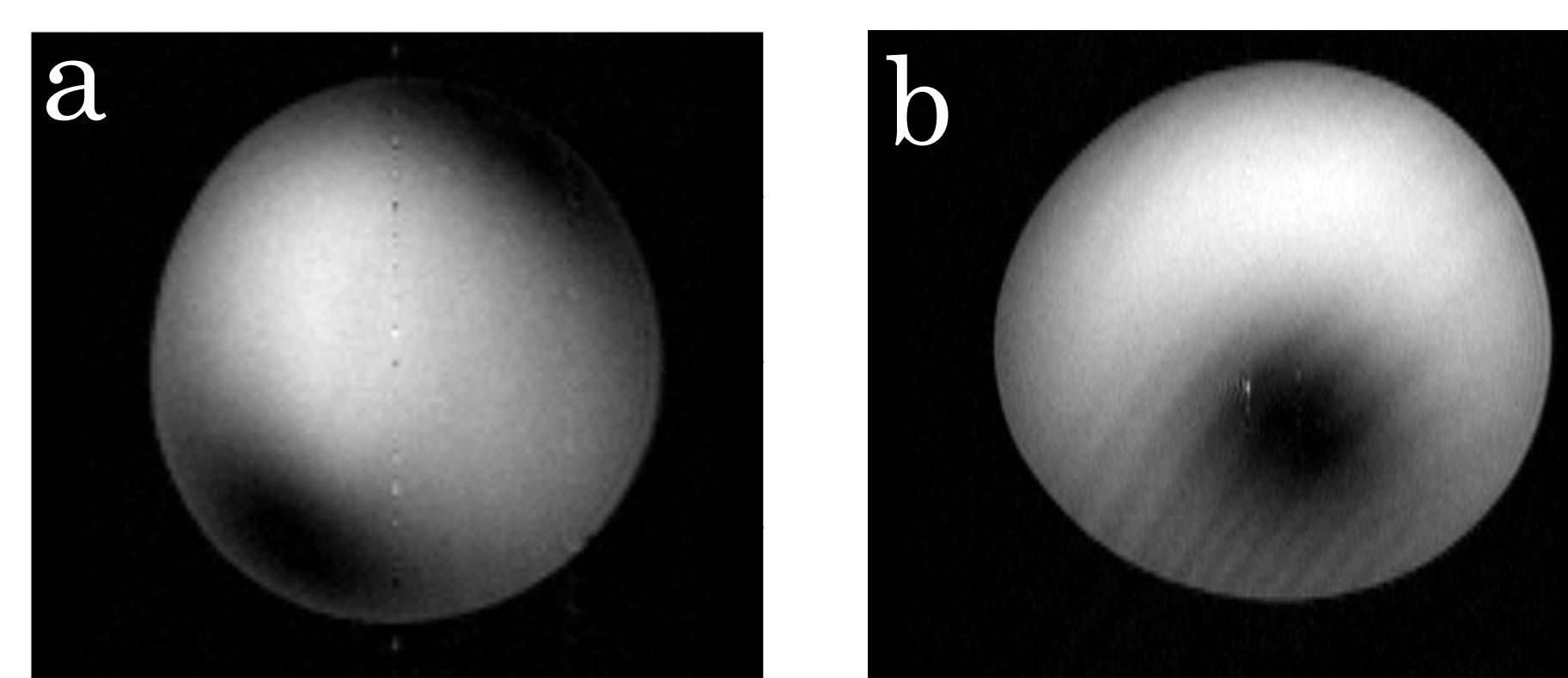


**Fig. 2: B<sub>1</sub> field maps in a partially filled dielectric waveguide.** (a,c) TE<sub>11</sub> mode and (b,d) TE<sub>01</sub> through coronal and axial slices, respectively.  $D_{rod}$  corresponds to the dielectric waveguide diameter (3.5 cm), and  $D_{mesh}$  is the diameter of the metallic waveguide (5.5 cm).

## Results:

- Mode selection can be accomplished by altering coil orientation with respect to  $B_0$ , i.e. either orthogonal or parallel  $B_1$  (see Fig.1)
- The orthogonal loop coil (Fig. 1b) results in images exhibiting a TE<sub>11</sub>-like mode (Figs. 3a and 4a)
- The parallel loop coil (Fig. 1a) results in images exhibiting a TE<sub>01</sub>-like mode (Figs. 3b and 4b)
- Compared to a 900-MHz birdcage coil (see Fig. 4c), the implemented waveguide technique provides an improved longitudinal coverage that is limited only by imaging gradient linearity



SNR = 43

SNR = 44

**Fig. 3: Axial images from multislice 2D GRE datasets for the 3.5-cm deionized water waveguide:** TE/TR = 5/500 ms, res. = 312x312  $\mu$ m, FOV = 4x4 cm, 1-mm slice thickness. (a) TE<sub>11</sub> mode acquired with the orthogonal loop; (b) TE<sub>01</sub> mode acquired with the parallel loop. The signal-to-noise ratio (SNR) was computed over the entire cylinder for this slice, including the nulls.

- To show the feasibility of tissue imaging, high resolution 3D datasets of an *ex vivo* preserved mouse head immersed in 0.9% saline were acquired (Fig. 5).

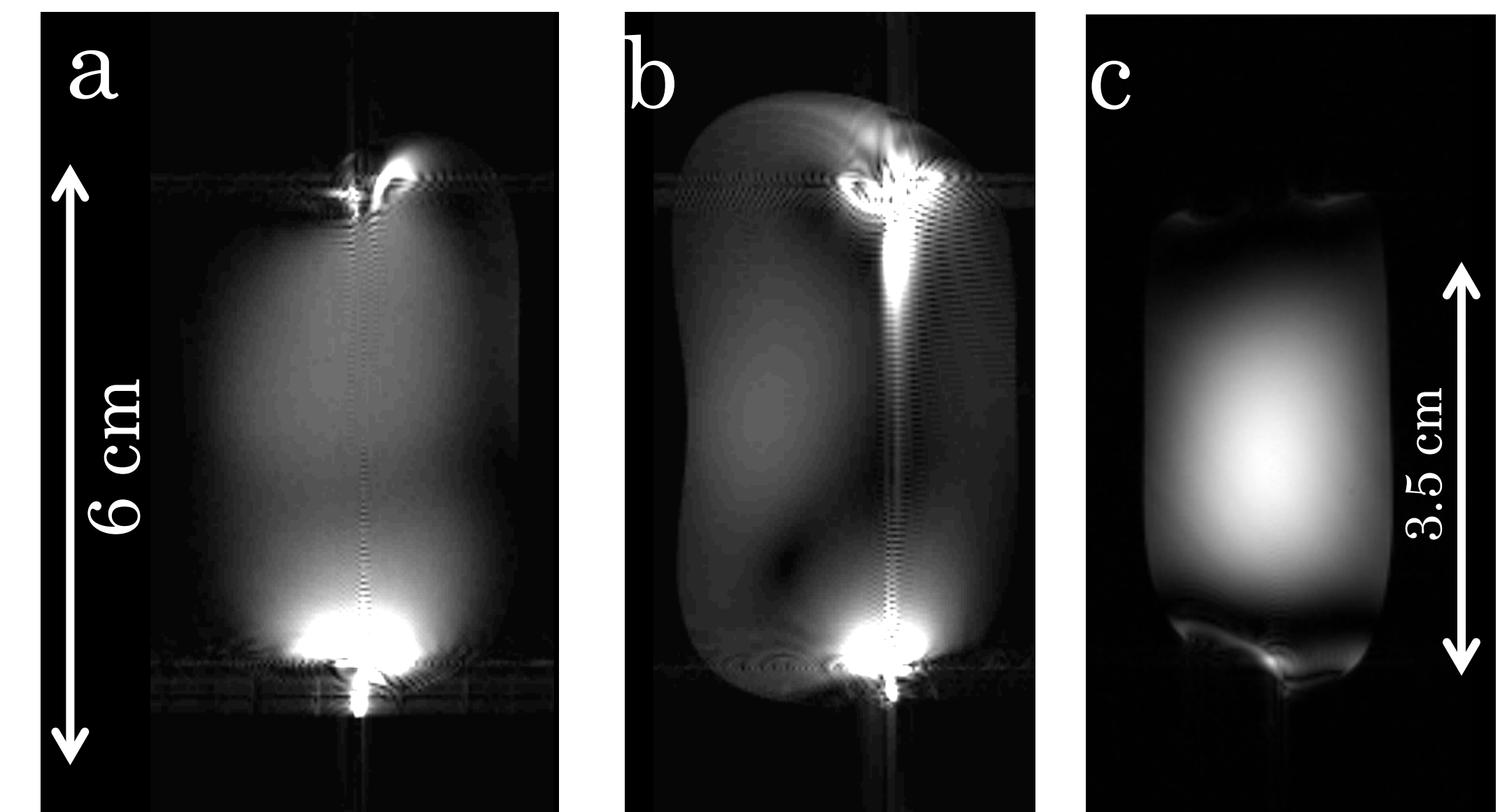


**Fig. 4: Coronal images from multislice 2D GRE datasets for the 3.5 cm deionized water waveguide:** TE/TR = 5/500 ms, res.=312x312  $\mu$ m, FOV = 8x4 cm, 1-mm slice. (a) TE<sub>11</sub> mode acquired with orthogonal loop; (b) TE<sub>01</sub> mode acquired with parallel loop; (c) Birdcage coil loaded with a polyethylene glycol sample.

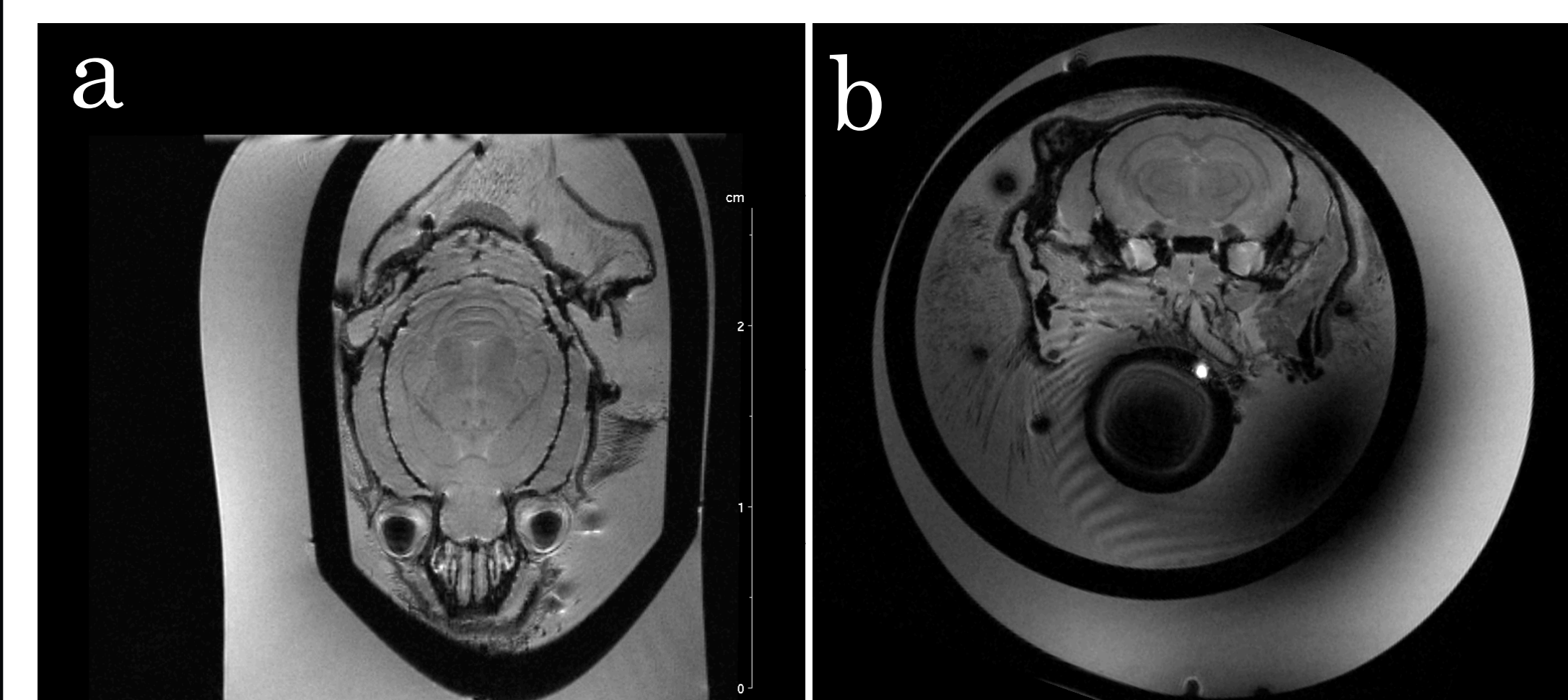


**Fig. 5: (a) Coronal and (b) axial images of a preserved mouse head from a 3D GRE dataset:** TE/TR=5/125 ms, iso. res.=100  $\mu$ m, FOV = 3.5x3.5x3.5 cm. Data was acquired with the parallel loop coil. Note TE<sub>01</sub> characteristic null in (b).

## Conclusions & Discussion:

- With the appropriate waveguide dielectric/diameter combination, traveling wave MRI can be achieved in ultra-high field vertical widebore systems.
- Mode selection was achieved via manipulation of waveguide coupling with different RF configurations, showing that non-TE<sub>11</sub> mode propagation is possible.
- RF simulations corroborate observed mode structures from MR images. However, in practice there exist mode asymmetries as well as hybrid HE<sub>nm</sub> modes.
- With increases in  $B_0$  field strength for clinical and pre-clinical systems, the impact of high dielectric materials for traveling wave MRI can become more significant.

## References & Acknowledgements:

- [1] Brunner, D.O. *et al.*, (2009). *Nature*, 457: 994-999  
 [2] Webb, A.G. *et al.*, (2010). *Magn Reson Med*, 63(2): 297-302  
 [3] Tonyushkin, A. *et al.*, (2011). *Proc. ISMRM* 19, p.1903  
 [4] Brunner, D.O. *et al.*, (2011). *Magn Reson Med*, 66: 290-300  
**MRI data were supported through and acquired at the NHMFL of The Florida State University (UCGP to SCG).**